Cooperative Beamforming for Wireless Ad Hoc Networks

Lun Dong, Athina P. Petropulu
Department of Electrical and Computer Engineering
Drexel University, Philadelphia, PA 19104

H. Vincent Poor
School of Engineering and Applied Science
Princeton University, Princeton, NJ 08544

***Abstract*—Via collaborative beamforming, nodes in a wireless network are able to transmit a common message over long distances in an energy efficient fashion. However, the process of making available the same message to all collaborating nodes introduces delays. In this paper, a MAC-PHY cross-layer scheme is proposed that enables collaborative beamforming at significantly reduced collaboration overhead. It consists of two phases. In the first phase, nodes transmit locally in a random access time-slotted fashion. Simultaneous transmissions from multiple source nodes are viewed as linear mixtures of all transmitted packets. In the second phase, a set of collaborating nodes, acting as a distributed antenna system, beamform the received analog waveform to one or more faraway destinations. This step requires multiplication of the received analog waveform by a complex weight, which is independently computed by each cooperating node, and which allows packets bound to the same destination to add coherently at the destination node. Assuming that each node has access to location information, the proposed scheme can achieve high throughput, which in certain cases exceeds one. An analysis of the symbol error probability corresponding to the proposed scheme is provided.**

I. Introduction

Transmission over long distances often requires significant amounts of energy in order to overcome attenuation. Energy is usually a scarce commodity in wireless ad hoc networks, as nodes typically operate on batteries, which in many cases are difficult to replace or recharge. Thus, energy-efficient schemes for long-distance transmission in wireless networks have recently been of much interest. In some such situations, multihop may be a preferred solution. However, there are several challenges in transmitting real-time services over multiple hops. For example, the traditional CSMA/CA based medium access control (MAC) for avoiding collisions does not work well in a multihop scenario because transmitters are often out of reach of other nodes' sensing ranges. Thus, packets traveling across the network experience interference and a large number of collisions, which introduce long delays. Also, multihop networks require a high node density which makes routing difficult and affects the reliability of links [1].

Recently, a collaborative beamforming technique was proposed in [3], in which randomly distributed nodes in a network cluster form an antenna array and beamform data to a faraway destination without each node exceeding its power constraint. The destination receives data with high signal power. Beamforming with antenna arrays is a well studied technology; it provides space-division multiple access (SDMA) which enables significant increases in communication rate. A challenge with implementing beamforming in ad hoc networks is that the geometry of the network may change dynamically. In [3], it was shown that randomly distributed nodes can achieve a nice average beampattern with a narrow main lobe and low side lobes. The directivity of the pattern increases as the number of collaborating nodes increases. Such an approach, when applied in the context of a multihop network reduces the number of hops needed, thereby reducing packet delays and improving throughput. However, to study network performance, one must take into account the information-sharing time that is required for node collaboration. If a time-division multiple-access (TDMA) scheme were to be employed, the information-sharing time would increase proportionally to the number of source nodes (i.e., the nodes having packets to transmit).

This work was supported by the National Science Foundation under Grants ANI-03-38807, CNS-06-25637 and CNS-04-35052, and by the Office of Naval Research under Grant N00014-07-1-0500.

In this paper we propose a scheme that is based on the idea of collaborative beamforming, and reduces the time required for information sharing. A preliminary version of the proposed scheme appeared in [4]. The work in this paper contains error analysis that provides insight into the performance of the proposed approach. The main idea is as follows. Different source nodes in the network are allowed to transmit simultaneously. Collaborating nodes receive linear mixtures of the transmitted packets. Subsequently, each collaborating node transmits a weighted version of its received signal. The weights are such that one or multiple beams are formed, each focusing on one destination node, and reinforcing the signal intended for a particular destination as compared to the other signals. Each collaborating node computes its weight based on the estimated channel coefficients between sources and itself. This scheme achieves higher throughput and lower delay with the cost of lower SINR as compared to [3]. In the preliminary version of this work [4], the analysis of interference at the receiving node was done asymptotically, i.e., as the number of collaborating nodes tends to infinity. Here we provide analytical expressions for symbol error probability (SEP) that directly depend on the number of collaborating nodes. The analysis shows how SEP is affected by transmission power, signal-to-noise ratio, number of simultaneously transmitting nodes and number of collaborating nodes.

II. Background on collaborative beamforming

For simplicity, let us assume that sources and destinations are coplanar. We index source nodes using a subscript i, with t_i denoting the i-th node. At slot n, one source node t_m needs to transmit the signal $s_m(n)$ to a faraway destination node q_m. Suppose that set of N nodes, designated as collaborating nodes $c_1, \ldots, c_N$, have access to $s_m(n)$. The locations of these collaborating nodes follow a uniform distribution over a disk of radius R. We denote the location of c_i in polar coordinates with respect to the origin of the disk by (r_i, ψ_i). Let $d_{im}(\phi_m)$, or simply d_{im}, represent the distance between c_i and the destination q_m, where ϕ_m is the azimuthal angle of q_m with respect to the origin of the disk. $d_{0m}(\phi_m)$ or d_{0m} denotes the distance between the origin of the disk and q_m, so the polar coordinates of q_m are (d_{0m}, ϕ_m). Moreover, let $d_i(\phi)$ denote the distance between c_i and some receiving point with polar coordinate (d_{0m}, ϕ). The initial phases at the collaborating nodes are set to

$$\Psi_i(\phi_m) = -\frac{2\pi}{\lambda} d_{im}(\phi_m), \; i = 1, ..., N \; . \tag{1}$$

This requires knowledge of distances (relative to wavelength λ) between nodes and destination, and applies to the closed-loop case [3]. Alternatively, the initial phase of node i can be

$$\Psi_i(\phi_m) = \frac{2\pi}{\lambda} r_i \cos(\phi_m - \psi_i) \tag{2}$$

which requires knowledge of the node's position relative to some common reference point, and corresponds to the open-loop case [3]. In both cases synchronization is needed, which can be achieved via the use of the Global Positioning System (GPS).

The path losses between collaborating nodes and destination are assumed to be identical for all nodes. The corresponding array factor given the collaborating nodes at radial coordinates $\mathbf{r} = [r_1, ..., r_N]$ and azimuthal coordinates $\boldsymbol{\psi} = [\psi_1, ..., \psi_N]$ at location with polar coordinate (d_{0m}, ϕ) is

$$F(\phi; m|\mathbf{r}, \boldsymbol{\psi}) \;\; = \;\; \frac{1}{N} \sum_{i=1}^{N} e^{j\Psi_i(\phi_m)} e^{j\frac{2\pi}{\lambda} d_i(\phi)} \; . \tag{3}$$

Under far-field assumptions, the array factor becomes [3]

$$F(\phi; m|\mathbf{r}, \boldsymbol{\psi}) \;\; = \;\; \frac{1}{N} \sum_{i=1}^{N} e^{j\alpha(\phi;\phi_m) z_i} \tag{4}$$

where $\alpha(\phi; \phi_m) = 4\pi(R/\lambda)\sin(\frac{1}{2}(\phi_m - \phi))$, and $z_i = (r_i/R)\sin(\psi_i - \frac{1}{2}(\phi_m + \phi))$. The random variable z_i has the following probability density function (pdf):

$$f_{z_i}(z) = \frac{2}{\pi}\sqrt{1 - z^2}, \quad -1 \le z \le 1 \; . \tag{5}$$

Finally, the average beampattern can be expressed as [3]

$$\begin{aligned} P_{\mathrm{av}}(\phi) &= E_z\{|F(\phi|\mathbf{z})|^2\} \\ &= \frac{1}{N} + \left(1 - \frac{1}{N}\right) \left| 2\frac{J_1(\alpha(\phi; \phi_m))}{\alpha(\phi; \phi_m)} \right|^2 \end{aligned} \tag{6}$$

where $J_1(.)$ is the first-order Bessel function of the first kind. When plotted as a function of ϕ, $P_{\mathrm{av}}(\phi)$ exhibits a main lobe around ϕ_m, and side lobes away from ϕ_m. It equals one in the target direction, and the sidelobe level approaches $1/N$ as the angle moves away from the target direction. The statistical properties of the beampattern were analyzed in [3], where it was shown that under ideal channel and system assumptions, directivity of order N can be achieved asymptotically with N sparsely distributed nodes.

As we have noted, all of the collaborating nodes must have the same information to implement beamforming. Thus, the source nodes need to share their information symbols with all collaborating nodes in advance. If a TDMA scheme were to be employed, the information-sharing time would increase proportionally to the number of source nodes. In the following, we propose a novel scheme to reduce the information-sharing time and also allow nodes in the network to transmit simultaneously.

III. The proposed scheme

Here we refine the model of [3], focusing more directly on the physical model for the signal, fading channel and noise. In addition to the above assumptions, we will further assume the following:

1) The network is divided into clusters, so that nodes in a cluster can hear each other. In each cluster there is a node designated as the cluster-head (CH). Nodes in a cluster do not need to transmit their packets through the CH.
2) A slotted packet system is considered, in which each packet requires one slot for its transmission. Perfect synchronization is assumed between nodes in the same cluster.
3) Nodes transmit packets consisting of phase-shift keying (PSK) symbols each having the same power σ_s^2. Also, nodes operate under half-duplex mode, i.e., they cannot receive while they are transmitting.
4) Communication takes place over flat fading channels. The channel gain during slot n between source t_i and collaborating node c_j is denoted by $a_{ij}(n)$. It does not change within one slot, but can change between slots. The channel gains are independent and identically distributed (i.i.d.) complex Gaussian random variables with zero means and variances σ_a^2 across both time and space, i.e., $a_{ij}(n) \sim \mathcal{CN}(0, \sigma_a^2)$.
5) The complex baseband-equivalent channel gain between nodes c_i and q_m is $b_{im} e^{j\frac{2\pi}{\lambda} d_{im}}$ [6], where b_{im} is the path loss. The distances between collaborating nodes and destinations are much greater than the maximum distance between source and collaborating nodes. Thus, b_{im} is assumed to be identical for all collaborating nodes and equals the path loss between the origin of the disk and the destination, denoted by b_m.

Suppose that cluster C contains J nodes. During slot n, source nodes $t_1, \ldots, t_K$ need to communicate with nodes $q_1, \ldots, q_K$ that belong to clusters $C_1, \ldots, C_K$, respectively.

The azimuthal angle of destination q_i is denoted by ϕ_i. The packet transmitted by node t_j consists of L symbols $\mathbf{s}_j(n) \triangleq [s_j(n;0),\dots,s_j(n;L-1)]$. Due to the broadcast nature of the wireless channel, non-source nodes in cluster C hear a collision, i.e., a linear combination of the transmitted symbols. More specifically, node c_i hears the signal

$$\mathbf{x}_i(n) = \sum_{j=1}^{K} a_{ji}(n)\mathbf{s}_j(n) + \mathbf{w}_i(n) \tag{7}$$

where $\mathbf{w}_i(n) = [w_i(n;0),\dots,w_i(n;L-1)]$ represents noise at the receiving node c_i. The noise is assumed to be of zero mean and with covariance matrix $\sigma_w^2 \mathbf{I}_L$, where $\mathbf{I}_L$ is an $L \times L$ identity matrix.

Once the CH establishes that there has been a transmission, it initiates a collaborative transmission period (CTP), by sending a control bit to all nodes, e.g., 1, via an error-free control channel. The CH will continue sending a 1 in the beginning of each subsequent slot until the CTP has been completed. The cluster nodes cannot transmit new packets until the CTP is over.

Let q_m denote the destination of $\mathbf{s}_m(n)$. In slot $n+m,\ m = 1,\dots,K$, each collaborating node c_i transmits the signal

$$\tilde{\mathbf{x}}_i(n+m) = \mathbf{x}_i(n)\mu_m a_{mi}^*(n) e^{\Psi_i(\phi_m)} \tag{8}$$

where μ_m is a scalar used to adjust the transmit power and is the same for all collaborating nodes. μ_m is of the order of $1/N$.

Collaborating nodes need to know which are source nodes and then estimate the channel between all source nodes and themselves. One possible way to implement this is to use orthogonal IDs, as discussed in [4], [2].

Also, collaborating nodes require the knowledge of their initial phases. In closed-loop mode, each collaborating node can independently synchronize itself to a beacon sent from the destination and adjusts its initial phase to it [3]. In open-loop mode, each collaborating node needs to know its relative position from a predetermined reference point (e.g. the origin of the disk) within the cluster, which can be achieved by the use of GPS. To obtain initial phases, collaborating nodes also require knowledge of the azimuths of the destinations so that the beams can be steered toward desired directions, which may be broadcast by the CH via a control channel.

Given the collaborating nodes at radial coordinates $\mathbf{r} = [r_1,...,r_N]$ and azimuthal coordinates $\boldsymbol{\psi} = [\psi_1,...,\psi_N]$, the received signal at an arbitrary location with polar coordinates (d_{0m},ϕ), is

$$\mathbf{y}(\phi;m|\mathbf{r},\boldsymbol{\psi}) = \sum_{i=1}^{N} b_m \tilde{\mathbf{x}}_i(n+m) e^{j\frac{2\pi}{\lambda}d_i(\phi)} + \mathbf{v}(n+m) \tag{9}$$

where $\mathbf{v}(n+m)$ represents noise at the receiver during slot $n+m$. The covariance matrix of $\mathbf{v}(n+m)$ equals $\sigma_v^2 \mathbf{I}_L$.

It was shown in [4] that, as $N \to \infty$ and omitting the noise, $\mathbf{y}(\phi_m;m|\mathbf{r},\boldsymbol{\psi}) \to N\mu_m b_m \sigma_a^2 \mathbf{s}_m(n)$. Thus, the destination node q_m receives a scaled version of $\mathbf{s}_m(n)$. The beamforming step is completed in K slots, reinforcing one source signal at a time.

Assuming that all of the K source packets have distinct destinations at different resolvable directions, multiple beams can be formed in one slot, each beam focusing on one direction and reinforcing one source signal. In the rest of the paper, for simplicity we will consider only the case in which a single beam is formed during slot $n+m$, focusing on destination q_m. The results obtained under this assumption can be readily extended to multiple simultaneous beams.

Taking into account the assumptions on channels and noise, the average beampattern was derived in [4]. Defining the throughput, T, as the average number of packets that are successfully transmitted in a time slot, we showed in [4] that $K/(1+K) \le T \le K/2$, which could be greater than 1. Also, in [4], we showed that under a fixed transmit power, the average signal-to-interference plus noise ratio (SINR) is asymptotically β' times less than that of [3], where $\beta' = K + 1 + \frac{\sigma_w^2}{\sigma_s^2\sigma_a^2}$.

IV. Symbol Error Probability (SEP)

In the following, for simplicity we omit the time index, and replace $\mathbf{y}$, $\tilde{\mathbf{x}}_i$, $\mathbf{x}_i$, $\mathbf{s}_i$, $\mathbf{w}_i$ and $\mathbf{v}$ in the above equations by y, $\tilde{x}_i$, x_i, s_i, w_i and v (i.e., with one of their samples) respectively.

Our analysis will be conditioned on K, the number of simultaneously transmitting nodes. In general, K is a random variable, whose distribution is a function of the traffic characteristics, e.g, traffic load, traffic distribution, transmission control scheme, etc. In the simple case in which each node transmits with identical probability P_t, K has a binomial distribution. Once the distribution of K is given then we can determine the SEP as $P_s = \sum_{K=1}^{J} P(K)P_s(K)$.

From (9), the received signal at the destination q_m is

$$y(\phi_m;m) = \mu_m b_m \sum_{i=1}^{N} |a_{mi}|^2 s_m + \mu_m b_m \sum_{i=1}^{N} a_{mi}^* (\sum_{\substack{j=1\\j\neq m}}^{K} a_{ji}s_j + w_i) + v \tag{10}$$

where the first term is the desired signal and the remaining terms represent interference and noise. Recall that $a_{ji} \sim \mathcal{CN}\left(0,\sigma_a^2\right)$. Since s_j is a PSK symbol, the magnitude of $a_{ji}s_j$ is $\sigma_s^2|a_{ji}|$ and its phase is still uniformly distributed in $[0,2\pi]$. Thus, $a_{ji}s_j \sim \mathcal{CN}\left(0,\sigma_a^2\sigma_s^2\right)$. Therefore,

$$\eta_i \triangleq \sum_{\substack{j=1\\j\neq m}}^{K} a_{ji}s_j + w_i \sim \mathcal{CN}\left(0,\sigma_\eta^2\right) \tag{11}$$

where $\sigma_\eta^2 \triangleq (K-1)\sigma_a^2\sigma_s^2 + \sigma_w^2$.

Given a_{mi}, the instantaneous SINR, γ, equals

$$\gamma = \frac{\mu_m^2 b_m^2 (\sum_{i=1}^{N}|a_{mi}|^2)^2 \sigma_s^2}{\mu_m^2 b_m^2 \sum_{i=1}^{N}|a_{mi}|^2 \sigma_\eta^2 + \sigma_v^2} = \frac{\mu_m^2 b_m^2 \xi^2 \sigma_s^2}{\mu_m^2 b_m^2 \xi \sigma_\eta^2 + \sigma_v^2} \tag{12}$$

where $\xi \triangleq \sum_{i=1}^{N}|a_{mi}|^2$.

Note that μ_m is of order $1/N$. As $N \to \infty$, $\mu_m^2 b_m^2 \xi \sigma_\eta^2 \to 0$, and γ reduces to $\mu_m^2 b_m^2 \xi^2 \sigma_s^2/\sigma_v^2$, which corresponds to the scenario of additive white Gaussian noise (AWGN). Thus, under certain transmit powers, no matter how large N is, the SEP of the proposed scheme is always lower bounded by the SEP under AWGN.

Since $|a_{mi}|$ is Rayleigh distributed, $\xi \sim \text{Erlang}(N, \sigma_a^2)$. The pdf of the Erlang distribution is

$$\text{Erlang}(k,\theta): \quad f(x;k,\theta) = \frac{x^{k-1}e^{-\frac{x}{\theta}}}{\theta^k (k-1)!}, \quad x \geq 0 \ . \tag{13}$$

The moment generating function (MGF) of γ is

$$\begin{aligned} \mathcal{M}_\gamma(s) &= \int_{-\infty}^{\infty} \exp(s\gamma) f_\xi(\xi) d\xi \\ &= \int_0^{\infty} \exp\left(\frac{s\mu_m^2 b_m^2 \xi^2 \sigma_s^2}{\mu_m^2 b_m^2 \xi \sigma_\eta^2 + \sigma_v^2}\right) \frac{\xi^{N-1} e^{-\frac{\xi}{\sigma_a^2}}}{\sigma_a^{2N}(N-1)!} d\xi \end{aligned} \tag{14}$$

based on which, the average SEP for M-PSK symbols is [5]

$$\begin{aligned} P_s(K) &= \frac{1}{\pi}\int_0^{\frac{(M-1)\pi}{M}} \mathcal{M}_\gamma\left(-\frac{\sin^2(\pi/M)}{\sin^2\varphi}\right) d\varphi \\ = &\ \frac{1}{\pi}\int_0^{\frac{(M-1)\pi}{M}} \int_0^{\infty} \exp\left(-\frac{\sin^2(\pi/M)}{\sin^2\varphi}\cdot \frac{\mu_m^2 b_m^2 \xi^2 \sigma_s^2}{\mu_m^2 b_m^2 \xi \sigma_\eta^2 + \sigma_v^2}\right) \\ &\times \frac{\xi^{N-1} e^{-\frac{\xi}{\sigma_a^2}}}{\sigma_a^{2N}(N-1)!} d\xi d\varphi \ . \end{aligned} \tag{15}$$

Since there is no closed-form expression for $\mathcal{M}_\gamma(s)$ or $P_s(K)$, in the following we will make some approximations to simplify the above expressions.

A. A Simple Bound for SEP

Let us fix an $\epsilon > 0$, and define ξ_0 such that $P(\xi \leq \xi_0) = \epsilon$. Also, let us define

$$\tilde{\gamma} \triangleq \frac{\mu_m^2 b_m^2 \xi^2 \sigma_s^2}{\mu_m^2 b_m^2 \xi \sigma_\eta^2 + \sigma_v^2 \xi/\xi_0} = \frac{\mu_m^2 b_m^2 \sigma_s^2}{\mu_m^2 b_m^2 \sigma_\eta^2 + \sigma_v^2/\xi_0} \cdot \xi \triangleq c_{\tilde{\gamma}} \xi \ . \tag{16}$$

When ϵ is small, it holds with probability $\geq 1-\epsilon$ that $\tilde{\gamma} \leq \gamma$. Since $c_{\tilde{\gamma}} > 0$ and s is negative in the range of interest, we can always find a small enough ϵ so that $\mathcal{M}_{\tilde{\gamma}}(s) \geq \mathcal{M}_\gamma(s)$.

Note that $\tilde{\gamma} \sim \text{Erlang}(N, \sigma_a^2 c_{\tilde{\gamma}})$ and thus the MGF of $\tilde{\gamma}$ is of the following simple form:

$$\mathcal{M}_{\tilde{\gamma}}(s) = (1 - s\sigma_a^2 c_{\tilde{\gamma}})^{-N} \ . \tag{17}$$

From (15), the SEP for M-PSK symbols based on $\tilde{\gamma}$ is

$$\tilde{P}_s(K) = \frac{1}{\pi}\int_0^{(M-1)\pi/M} \left(1 + \frac{\sin^2(\frac{\pi}{M})\sigma_a^2 c_{\tilde{\gamma}}}{\sin^2\varphi}\right)^{-N} d\varphi \ . \tag{18}$$

Defining $c \triangleq \sin^2(\frac{\pi}{M})\sigma_a^2 c_{\tilde{\gamma}}$, and using the result of Eq. (5A.17) in [5] we obtain

$$\begin{aligned} \tilde{P}_s(K) &= \frac{1}{\pi}\int_0^{(M-1)\pi/M} \left(1 + \frac{c}{\sin^2\varphi}\right)^{-N} d\varphi \\ &= \frac{M-1}{M} - \frac{1}{\pi}\sqrt{\frac{c}{1+c}}\Big\{\left(\frac{\pi}{2} + \tan^{-1}\zeta\right)\sum_{n=0}^{N-1}\binom{2n}{n}\frac{1}{[4(1+c)]^n} \\ &\quad + \sin(\tan^{-1}\zeta)\sum_{n=1}^{N-1}\sum_{j=1}^{n}\frac{T_{jn}}{(1+c)^n}[\cos(\tan^{-1}\zeta)]^{2(n-j)+1}\Big\} \end{aligned} \tag{19}$$

where

$$\zeta \triangleq \sqrt{\frac{c}{1+c}}\cot\left(\frac{\pi}{M}\right) \tag{20}$$

and

$$T_{jn} \triangleq \frac{\binom{2n}{n}}{\binom{2(n-j)}{n-j} 4^j [2(n-j)+1]} \ . \tag{21}$$

Recalling that $\mathcal{M}_{\tilde{\gamma}}(s) \geq \mathcal{M}_\gamma(s) \geq 0$, we have $\tilde{P}_s(K) \geq P_s(K)$. The result of (19) is an upper bound of the exact SEP of (15).

An even simpler upper bound for $\tilde{P}_s(K)$ can be obtained based on Eq. (5A.76) of [5]:

$$\tilde{P}_s(K) \leq \frac{M-1}{M}\left(1 + \frac{c}{\sin^2(\frac{(M-1)\pi}{M})}\right)^{-N} \tag{22}$$

which for BPSK becomes

$$\tilde{P}_s(K) \leq \frac{1}{2}\left(1 + \sigma_a^2 c_{\tilde{\gamma}}\right)^{-N} \ . \tag{23}$$

Remark: As $\mu_m \to \infty$, $c_{\tilde{\gamma}}$ reduces to σ_s^2/σ_η^2, in which case the corresponding result of (19) can be viewed as a lower bound when the transmit power of collaborating nodes approaches infinity. It shows that no matter how large the transmit power is, the SEP can never be smaller than this bound. The SEP floor is a result of the interference from other source nodes. To achieve lower SEP for a given K, one must increase N. Based on (22), this bound decreases approximately in a power-law fashion as N increases.

V. SIMULATIONS

In this section, we study the SEP performance of the proposed method via simulations, and also via the proposed analytical expressions.

We assume the channels among nodes in a cluster are selected from zero-mean complex Gaussian processes, which are constant within one slot, but vary between slots. Let us define $\gamma_1 \triangleq \sigma_s^2\sigma_a^2/\sigma_w^2$, which represents the average SNR in the process of information sharing, and define $\gamma_2 \triangleq N^2\mu_m^2 b_m^2 \sigma_s^2 \sigma_a^4/\sigma_v^2$ to represent the asymptotic average SNR (when $N \to \infty$) at the receiver. Note that γ_2 is independent of N since μ_m is of the order of $1/N$. Eq. (12) can be rewritten by

$$\gamma = \frac{\tilde{\xi}^2/N^2}{\frac{K-1+\gamma_1^{-1}}{N^2}\tilde{\xi} + \gamma_2^{-1}} \tag{24}$$

where $\tilde{\xi} = \xi/\sigma_a^2 \sim \mathrm{Erlang}(N, 1)$. Then, the SINR is determined only by γ_1, γ_2, K and N. Each packet contains BPSK symbols, so SEP is equivalent to BER. We take $\epsilon = 0.01$. Also, we assume perfect knowledge of channels, number of source nodes and destination information. Only one beampattern is formed in each slot. For simulation-based BER, we perform a Monte-Carlo experiment consisting of 10^6 repeated independent trials.

Fig. 1 shows the BER versus γ_2 estimated from the network simulation ($\circ$ line) when $K = 4$ nodes transmit all the time. The parameter γ_1 is fixed at 20 dB. The estimated BER is in perfect agreement with the analytical result for the exact SEP of (15)("$*$" line); in fact the two lines are indistinguishable. The upper bound on the exact SEP, computed by (19), is shown as the solid line. One can see that $\epsilon = 0.01$ can guarantee a tight bound under various parameters and SNR ranges. The simple upper bound computed via (23) is also shown (dashed lines).

Extensive simulations confirm that the simulation-based BER and analytical SEP match well under a wide variety of scenarios. Thus, in the following we will simply use the analytical result of (15) to study the performance of the proposed method.

Fig. 2 shows how the BER depends on the number of collaborating nodes for $\gamma_1 = 20$ dB and different values of γ_2. Fig. 3 shows how K affects BER, where $\gamma_1 = \gamma_2 = 20$ dB. As K increases, the SEP increases. Fig. 4 shows how BER changes with γ_1, where $\gamma_2 = 20$ dB and $K = 4$. Recall that $\sigma_\eta^2 = \sigma_a^2\sigma_s^2(K - 1 + \gamma_1^{-1})$. K plays a dominant role in the interference (when $K > 1$). As observed in Fig. 4, the SEP decreases only slightly with the increase of γ_1.

VI. Conclusions

We have proposed a scheme for wireless ad hoc networks that uses the idea of collaborative beamforming and at the same time reduces the time needed for information sharing during the collaborative phase. We have provided an analysis of the SEP, which shows how the performance depends on the number of collaborating nodes, the number of simultaneously source users and noise levels at collaborating nodes and the final destination node.

References

[1] H. Gharavi and K. Ban, "Multihop sensor network design for wide-band communications," *Proc. IEEE*, vol. 91, no. 8, pp. 1221 - 1234, Aug. 2003.

[2] R. Lin and A. P. Petropulu, "New wireless medium access protocol based on cooperation," *IEEE Trans. Signal Process.*, vol. 53, no 12, pp. 4675 - 4684, Dec. 2005.

[3] H. Ochiai, P. Mitran, H. V. Poor and V. Tarokh, "Collaborative beamforming for distributed wireless ad hoc sensor networks", *IEEE Trans. Signal Process.*, vol. 53, no. 11, pp. 4110 - 4124, Nov. 2005.

[4] A. P. Petropulu, L. Dong and H. V. Poor, "A high-throughput cross-layer scheme for distributed wireless ad hoc networks," *Proc. Conference on Information Sciences and Systems*, Baltimore MD, Mar. 2007.

[5] M. K. Simon and M.-S. Alouini, *Digital Communication over Fading Channels (second edition).* John Wiley & Sons, New York, 2005.

[6] D. Tse and P. Viswanath, *Fundamentals of Wireless Communication.* Cambridge Univ Press, Cambridge, UK, 2005.

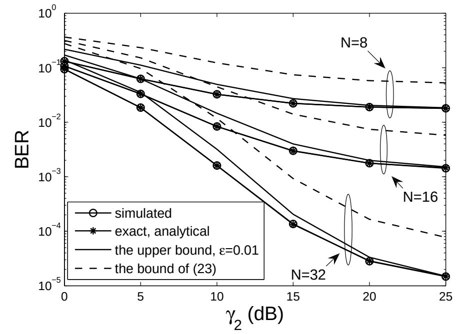

Fig. 1. BER vs. γ_2 ($K = 4, \gamma_1 = 20$ dB); $N = 8, 16, 32$; empirical results, analytical exact results and upper bounds.

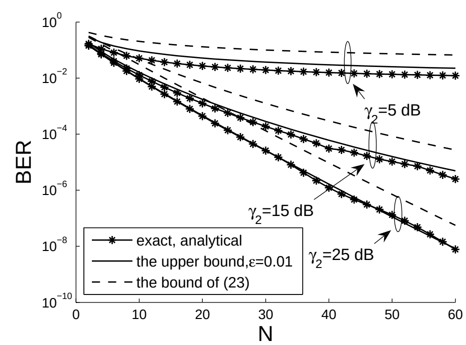

Fig. 2. BER vs. N ($K = 4, \gamma_1 = 20$ dB); $N = 8, 16, 32$; analytical exact results and upper bounds.

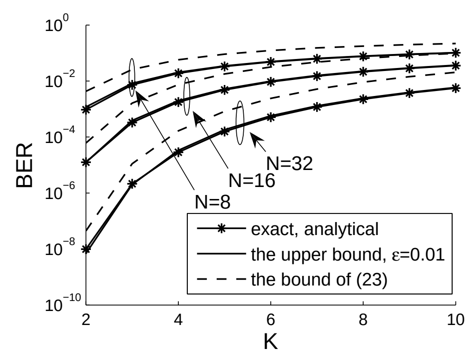

Fig. 3. BER vs. K ($\gamma_1 = \gamma_2 = 20$ dB); $N = 8, 16, 32$; analytical exact results and upper bounds.

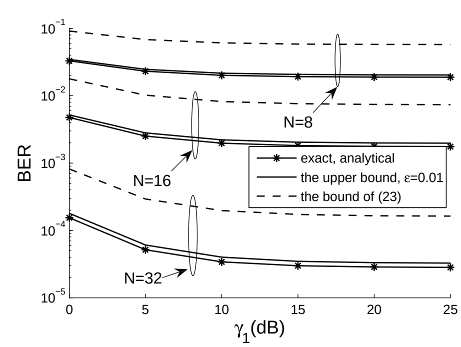

Fig. 4. BER vs. γ_1 ($K = 4, \gamma_2 = 20$dB); $N = 8, 16, 32$; analytical exact results and upper bounds.